MODELING OF BENDING MAGNETS FOR SIRIUS

X.R. Resende, R. Basílio, L. Liu, P.P. Sanchez and G. Tosin

LNLS – Laboratório Nacional de Luz Síncrotron, CP 6192, 13084-970, Campinas, SP, Brazil

Abstract

The new Brazilian synchrotron source, Sirius, will be a 3 GeV storage ring with a triple bend lattice with a minimum emittance of 1.7 nm rad. The ring dipoles are excited with permanent magnets. The middle bend has a small 1.4 degree slice in its center with 1.94 T field and serve as an additional hard X-ray source with critical energy of 11.6 keV. Other bending magnets have low 0.50 T field with gradients, allowing for a further emittance reduction. The bending slice shows a longitudinal profile with no uniform field plateau and with long-range fringe fields which are coupled with the fields of neighbouring dipoles. To take into account the interaction of the field-intersecting dipoles, realistic 3D models of the magnets have been created and their field configuration solved using finite element techniques. Field maps calculated from the 3D magnet models were used for the construction of segmented models of bend elements in beam dynamics codes.

INTRODUCTION

The magnet lattice chosen for Sirius is a 20-cell modified triple-bend-achromat (TBA) with the relatively low field of 0.50 T for the main deflection dipoles. Despite the low bending field, a modification in the lattice allows for hard x-rays from dipoles: the middle bending magnet is split to accommodate a high field thin dipole of 1.94 T in its center, as shown in Figure 1.
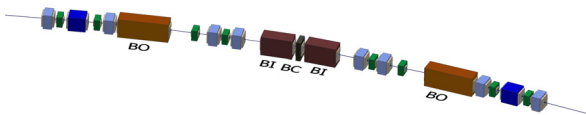
Figure 1: Sirius chromatic arc with two 0.50 T outer dipoles (BO), two 0.50 T inner dipoles (BI) and one 1.94 T thin slice dipole in the center (BC).

Each BO nominally deflects the beam in 5º, leaving 8º for the inner and center dipoles. BC dipoles are very short and their fields leak out to the neighbouring BI dipoles. The full gap of all dipoles is 35 mm. Basic dipole parameters are listed in Table 1. In addition, BI and BO will have powered coils for small field trimming.

Although for initial lattice design hard-edge uniform field models for dipoles were used, more elaborated versions were needed so that the impact of the unusually short BC dipole and its proximity to BI dipole could be ascertained in a systematic manner. Furthermore, the low field permanent magnet dipoles will be rectangular in shape, not curved. This means that the field gradient of the defocusing BI and BO dipoles will be perpendicular to the longitudinal axis, not to the beam reference trajectory. As a result, neither the vertical field component B_y nor its gradient dB_y/dx will appear exactly constant to the particles. Apart from these first order effects, the central high field thin dipole BC model also presented a strong sextupole component that affects the dynamic aperture optimization.

Table 1: Basic dipole parameters of Sirius

	BC	BI	BO
Length [mm]	165	1100	1750
Field [T]	1.94	0.5	0.5
Gradient [T/m]	0	2.17	2.17
Deflection Angle [º]	1.4	3.3	5.0
Sagitta [mm]	0.5	7.9	19.1

3D MAGNET FIELD SIMULATIONS

In order to generate dipole field models for the lattice design and optimization codes that included fringe field and non-constant gradient effects, midplane field maps were computed and used. These maps were generated from 3D magnetic simulations performed with software MagNet[1] by the magnets group (Figure 2).
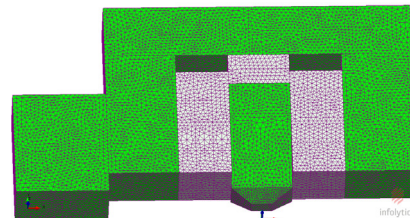
Figure 2: Simulation of one-quarter BC dipole with its finite-element mesh grid displayed. Steel material is coloured in green and NdFeB in gray.

Dipoles BI and BO were modelled with carbon steel 1010 and with an excitation curve taken from the software's materials database. As for BC dipoles, the material considered was carbon steel 1006 with an excitation curve measured from a sample lot.

For all dipoles, the excitation sources are NdFeB blocks simulated at 20 ºC with $B_r = 1.30$T for BI and BO and $B_r = 1.31$T for BC. These numbers are based on Helmholtz coils measurements.

The field maps generated from simulations contain all three field components tabulated on midplane and therefore should, apart from numerical artefacts due to the discretization of the grids in the maps, allow in principle for complete determination of the 3D magnetic fields and beam dynamics within gap regions of the dipoles. Grids used for these field maps had typically 0.5 mm longitudinal and horizontal point spacings.

Dipole Interaction

One of the first concerning issues in modeling the dipoles was the magnetic interaction between close neighbouring BI and BC. Independent magnets were simulated and their field maps were added and compared to a field map calculated from a simulation in which BI and BC interaction was taken into account (Figure 3).
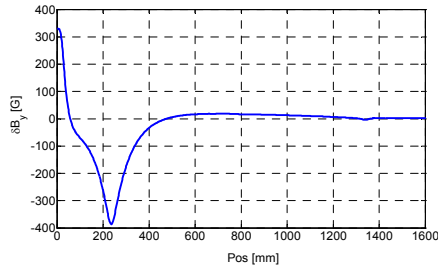
Figure 3: Magnetic interaction contribution to the BC/BI dipole field along the trajectory path.

The magnetic interaction can account for a field difference larger than 300 G at the center of the BC and close to the middle point between dipoles. The integrated difference, converted to deflection angle, is roughly -0.04º, corresponding to an error of 0.5%. This value is one order of magnitude larger than the current tolerance specification for steering error. In summary, the magnetic interaction between BC and BI is not negligible, justifying modeling these three dipoles as a single unit.

TRACKING MODELS

BC/BI Relative Positioning

The initial positions of the BC and BI dipoles were calculated based on the beam trajectory of independent hard-edge dipole models. Then a 3D magnetic simulation was done for the combined BC/BI dipoles and the generated field map was used to calculate the beam trajectory using Matlab's Runge-Kutta (RK) solver [2]. The positions of the dipoles in the model were adjusted in order for the trajectory to be centered as best as possible in the good-field region of the dipoles. The 3D magnetic simulation with the new dipoles' positions was performed again and its field map recalculated. This procedure was iterated 6 times before convergence was achieved. In between iterations, small model corrections were sometimes needed to ensure attaining the total nominal deflection angle of 8º and an integrated gradient of -5.2 T/m. At the end this procedure resulted in a 3D magnetic model of the combined dipoles, a centered reference trajectory and a midplane field map.

Model Segmentation

Next step was the construction of symplectic models for BO and BC/BI dipoles that could be used in beam dynamics studies and that accurately described: a) the correct equilibrium beam parameters, b) the linear and c) the non-linear beam dynamics. For this the vertical B_y field profile along the reference trajectory was segmented

and each segment represented by a hard-edge model with the same integrated field. This guaranties a proper model for the total dipole deflection angle. A segmentation algorithm was implemented that kept the error in the integral of B_y^2 smaller than a defined level.
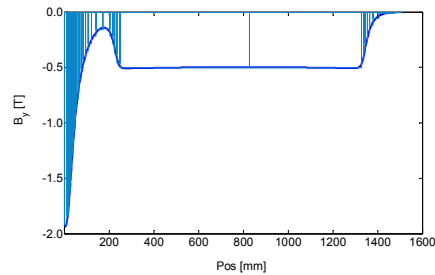
Figure 4: Dipoles BI and BC (half) field profiles and the corresponding longitudinal model segmentation.

This algorithm sets the number of segmentations in the model that, in conjunction with the choice of its length, define the accuracy of the calculated radiation integrals. This way, dipole BO was modelled with 32 hard-edge segments whereas BC/BI was modelled with 76 segments, as is shown in Figure 4 and in Figure 5.
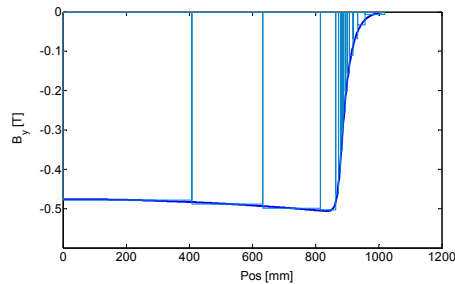
Figure 5: Half BO dipole field profile and its longitudinal model segmentation.

Multipoles

The quadrupole and higher order multipole components profiles were obtained from polynomial fit to the B_y field as a function of the perpendicular displacement in each point along the RK calculated reference trajectory. Fitting was done up to the 14-pole component and within a displacement interval of $\pm$ 6mm, corresponding to the scaled dynamic aperture of the bare optics at the locations of the dipoles.

Table 2: Integrated and normalized multipoles extracted from the field maps [$M_n = (1/n!)\, d^nB/dx^n\, L\, / \, (B\rho)_0$]

Multipole	BC/BI	BO
quadrupole [1]	-5.2E-1	-3.9E-1
sextupole [m^{-1}]	-2.4E+0	+9.9E-3
octupole [m^{-2}]	-1.6E+0	+1.4E+0
decapole [m^{-3}]	-4.4E+3	-1.6E+2
duodecapole [m^{-4}]	+4.8E+4	+3.3E+4
14-pole [m^{-5}]	+2.4E+7	+2.1E+6

Multipole longitudinal profiles are displayed in Figure 6 for the BC/BI dipoles set. To achieve a peak field of 1.94 T with a small deflection angle the three-dimensional optimization of the BC pole (see chamfered poles in Figure 2) lead to a rather strong sextupole. As mentioned before, this sextupole was considered in the non-linear dynamics optimization of the lattice.
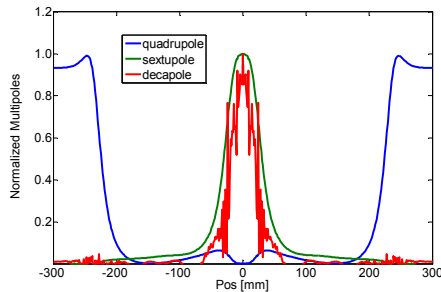
Figure 6: Profiles of the most important BC/BI multipoles fitted on the reference trajectory points.

The multipoles are then integrated along the reference trajectory for each model segment and used in the simulation codes.

Transfer Maps and Optical Functions

Transfer-map comparisons between RK integration of the equations of motion and tracking calculations through segmented models using Accelerator Toolbox[3] (AT) were performed. AT models replicate RK transfer maps very well all over the dynamic aperture range. Results for the BC/BI dipoles are displayed in Figure 7. Discrepancies are small, of the order of 4 µrad in angle and 0.8 µm in displacement for BC/BI, and 1.6 µrad and 0.4 µm for the BO dipole.
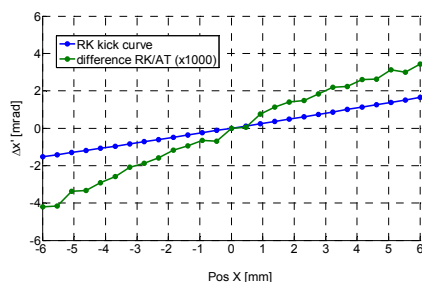
Figure 7: Horizontal kick of the BC/BI dipoles transfer map. Difference between RK and AT calculations is depicted in the green curve.

Optical functions were also analysed. Their values at the centers of dipoles BC and BO, as given from the lattice model, were propagated with transfer matrices calculated numerically with RK. They were compared with corresponding values calculated with AT and the agreement is also good, as seen in Figure 8, for the case of BC/BI dipoles set.

Radiation Integrals

Finally comparisons between radiation integrals calculated with optical functions and curvature radius

from AT and RK were done. Again, with fine segmented models for the dipoles the agreement is rather satisfactory. All discrepancies were below an acceptable level of 10% (Table 3). For example, the AT segmented model yields a natural emittance only 2.8% below the more precise value obtained with RK from field maps, which is 1.79 nm.rad.
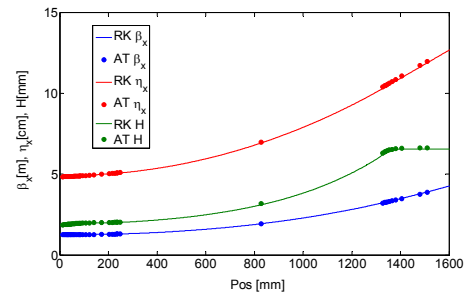
Figure 8: Optical functions in the BC/BI bends as calculated from RK tracking (solid lines) and with the AT model (circles).

Table 3: Radiation Integrals as given by AT models. Values quoted in parenthesis are discrepancies between corresponding AT and RK integrals

Rad.Int.	BC/BI	(%)	BO	(%)
I1 [m]	+9.17E-3	(**-1.7**)	+4.21E-3	(**+1.0**)
I2 [m^{-1}]	+8.09E-3	(**-5.8**)	+4.21E-3	(**+0.4**)
I3 [m^{-2}]	+6.68E-4	(**-8.5**)	+2.05E-4	(**+0.8**)
I4 [m^{-1}]	-3.52E-3	(**-0.9**)	-1.83E-3	(**+1.2**)
I5 [m^{-1}]	+1.64E-6	(**-7.8**)	+6.77E-7	(**+0.9**)

FINAL REMARKS

In summary, a set of tools for constructing fairly detailed and precise symplectic models for dipoles has been implemented and tested. These models constructed from field maps and RK integration yield controllable and accurate predicted values for beam equilibrium parameters, linear optics and multipoles and they can be used for studying long-term beam stability and injection efficiency. In principle this procedure could be applied to build models out of detailed 3D magnetic simulations for other elements as well whenever it is not clear how longitudinally-dependent effects (like fringe-fields, for example) should be taken into account or when an accuracy beyond implicit thin-lens approximation (as in the case of insertion device kick maps) is sought.

An additional lot of permanent magnets has been purchased and its NdFeB blocks are currently being characterized. A 2nd generation of dipole prototypes is scheduled to be built and tested before the end of 2012.

REFERENCES

[1]   MagNet v7, http://www.infolytica.com
[2]   ODE45 Solver, MATLAB, http://www.mathworks.com
[3]   A. Terebilo, RPAH314, PAC2001, Chicago.